



ELSEVIER

Contents lists available at ScienceDirect

Materials Letters

journal homepage: www.elsevier.com/locate/matlet

Growth of titanium dioxide nanorod arrays through the aqueous chemical route under a novel and facile low-cost method

M.M. Yusoff^{a,d}, M.H. Mamat^{a,b,*}, M.F. Malek^{a,b}, A.B. Suriani^c, A. Mohamed^c, M.K. Ahmad^e, Salman A.H. Alrokayan^f, Haseeb A. Khan^f, M. Rusop^{a,b}

^a NANO-ElecTronic Centre (NET), Faculty of Electrical Engineering, Universiti Teknologi MARA (UiTM), 40450 Shah Alam, Selangor, Malaysia

^b NANO-SciTech Centre (NST), Institute of Science (IOS), Universiti Teknologi MARA (UiTM), 40450 Shah Alam, Selangor, Malaysia

^c Nanotechnology Research Centre, Faculty of Science and Mathematics, Universiti Pendidikan Sultan Idris, Tanjung Malim, Perak 35900, Malaysia

^d Kuliyah of Engineering, International Islamic University Malaysia (IIUM), 50728 Kuala Lumpur, Malaysia

^e Microelectronic and Nanotechnology-Shamsuddin Research Centre (MiNT-SRC), Faculty of Electrical and Electronic Engineering, Universiti Tun Hussein Onn Malaysia (UTHM), 86400 Batu Pahat, Johor, Malaysia

^f College of Science, King Saud University (KSU), Riyadh 11451, Saudi Arabia

ARTICLE INFO

Article history:

Received 1 October 2015

Received in revised form

30 October 2015

Accepted 4 November 2015

Available online 5 November 2015

Keywords:

Semiconductors

TiO₂ Nanorod

Aqueous chemical route

Photosensor

Optical materials and properties

Electronic materials

ABSTRACT

Titanium dioxide (TiO₂) nanorod arrays were successfully synthesized through a facile aqueous chemical route on a fluorine tin oxide-coated glass substrate in a Schott bottle with cap clamps. Distinct rutile-phase TiO₂ peaks were observed via X-ray diffraction and micro-Raman spectroscopy. The surface morphology depicted in field-emission scanning electron microscopy and atomic force microscopy images showed that the nanorod arrays were successfully synthesized on the substrate. Moreover, these arrays possessed an average diameter of 120 nm and an average length of 1.52 μm. The prepared TiO₂ nanorod arrays exhibited high absorbance properties in the ultraviolet (UV) region (< 400 nm). In this study, the synthesized arrays may be applied in optical sensing based on the steady photocurrent results obtained under UV irradiation in a sodium sulfate electrolyte solution.

© 2015 Elsevier B.V. All rights reserved.

1. Introduction

The optical, electrical, and photochemical properties of nanostructured titanium dioxide (TiO₂) are unique and outstanding; this material has gained significant interest over the previous decade as an alternative material for photocatalysts [1] and electronic devices [2]. Numerous deposition methods have been examined for nanostructured TiO₂ synthesis, including sputtering, chemical vapor deposition, pulsed-laser deposition, and solution-based methods. Various studies on solution-based methods have attempted to extend the deposition process to synthesize a preferred nanorod array structure of the TiO₂ layer given the high surface area-to-volume ratio [3,4]. However, the process requires a high-pressure vessel or autoclave even at a low synthesis temperature. The main purpose of our research is to develop a fast, low-cost, and reliable solution-based method to prepare TiO₂

nanorod arrays for photosensor use.

In the present study, we propose a novel aqueous chemical route that uses a facile Schott bottle with cap clamps to produce an aligned TiO₂ nanorod array structure. This bottle has never been used for the dissolution condensation growth of TiO₂ nanorod arrays because the bottle cap is incapable of compressing the increasing pressure at elevated temperatures. Thus, cap clamps are introduced for clenching purposes. This low-cost, simple, yet fast method facilitates rapid progression and extensive study on the one-dimensional growth of a TiO₂ nanorod array structure. Finally, the synthesized arrays are characterized in terms of its structural, optical, and electrical properties.

2. Experimental

A fluorine tin oxide (FTO)-coated glass substrate was used for the growth of the TiO₂ nanorod arrays. The substrates were cleaned with acetone, ethanol, and deionized (DI) water in an ultrasonic bath. The hydrothermal process was performed for 10 min in a Schott bottle containing a mixture of hydrochloric

* Corresponding author at: NANO-ElecTronic Centre (NET), Faculty of Electrical Engineering, Universiti Teknologi MARA (UiTM), 40450 Shah Alam, Selangor, Malaysia.

E-mail address: mhmamat@salam.uitm.edu.my (M.H. Mamat).

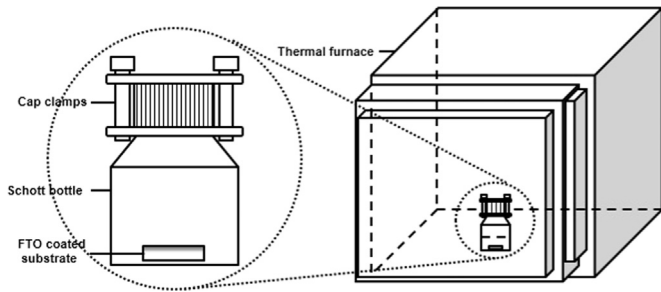


Fig. 1. Setup for TiO₂ nanorod array synthesis in a Schott bottle with cap clamps.

(HCl) acid and deionized water in a 1:1 volume ratio. Titanium (iv) butoxide (0.07 M) was added to the solution under vigorous stirring for another 30 min. A cleaned FTO-coated glass substrate was incorporated into the resultant transparent solution with the conducting side facing upward; then, the Schott bottle was sealed and fastened with cap clamps to retain the high pressure inside the bottle for 2 h at 150 °C. A schematic of this process is shown in Fig. 1. The synthesized sample on the substrate was then rinsed with DI water and dried at room temperature. Subsequently, the sample was annealed in a furnace at 450 °C for 30 min to improve crystallinity.

The morphology, topology, and crystallinity of the synthesized TiO₂ samples were observed via field-emission scanning electron microscopy (FESEM, ZEISS Supra 40VP), atomic force microscopy (AFM, Park System), and X-ray diffraction (XRD, Shimadzu XRD-6000), respectively. The sample was also characterized through micro-Raman spectroscopy (Renishaw InVia microRaman System, 514 nm laser). An ultraviolet–visible (UV–vis) spectrophotometer (Cary 5000) was used to characterize the optical properties of the synthesized TiO₂ nanorod arrays at wavelengths of 200–800 nm, whereas the electrical properties of these arrays were characterized with a direct current (DC) two-probing system (Advantest R6243) to identify the current–voltage (*I–V*) characteristic. The photocurrent was measured under UV irradiation using a two-probe measurement system (Keithley 2400) and a UV lamp (365 nm, 4 W) with a bias voltage of 1 V.

3. Results and discussion

The surface morphology depicted in Fig. 2(a) and (b) reflects the top view of the synthesized TiO₂ at magnifications of 100,000 \times and 30,000 \times , respectively. The nanorods, which display an average diameter of approximately 120 nm, were uniformly deposited on the substrate with dense arrays. Fig. 2

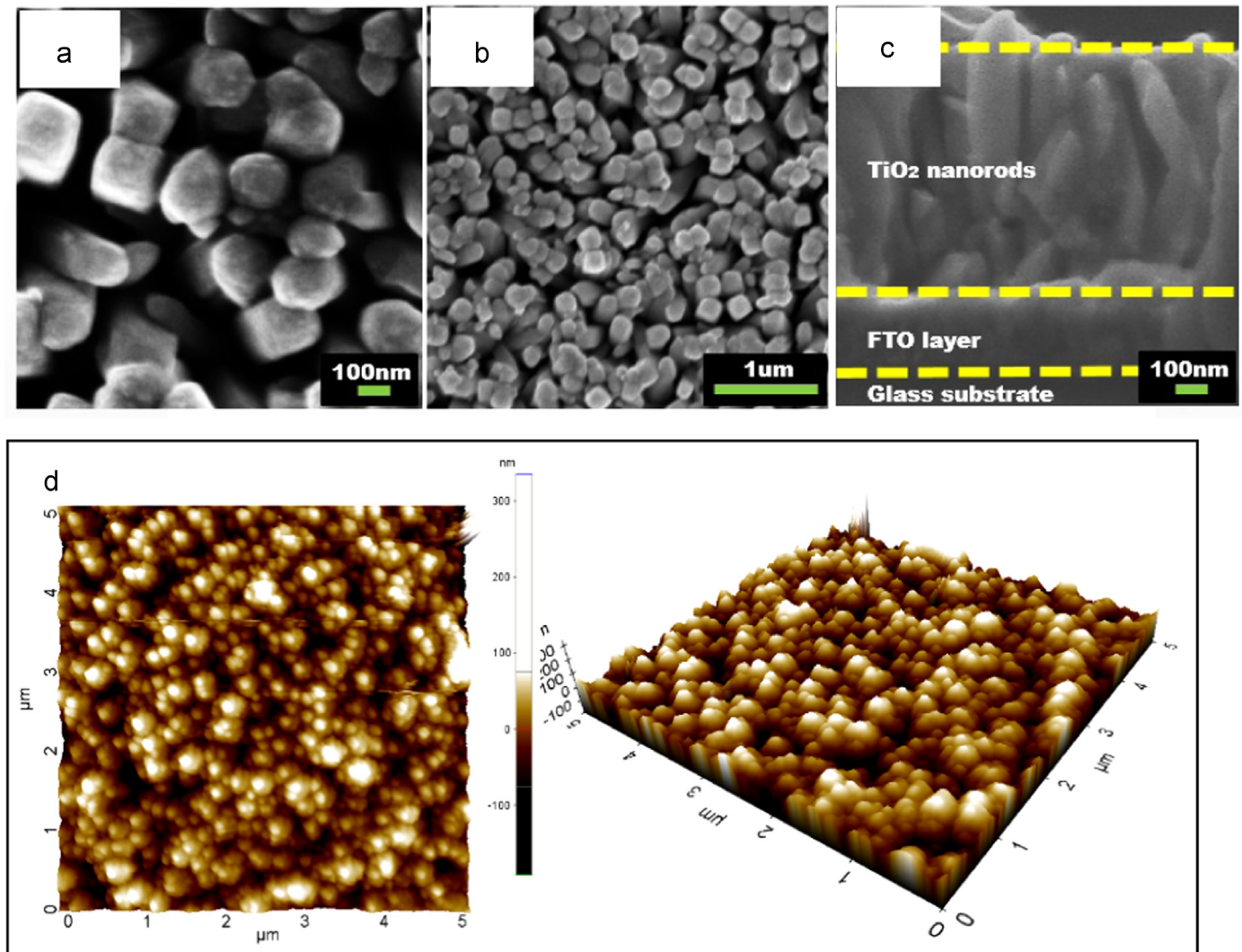


Fig. 2. FESEM images of the TiO₂ nanorod arrays at magnifications of (a) 100,000 \times and (b) 30,000 \times . (c) Cross-sectional and (d) AFM images of the synthesized TiO₂ nanorod arrays.

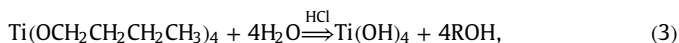
(c) displays a cross-sectional image of synthesized TiO₂ nanorod arrays on the FTO-coated glass substrate and indicates that the growth of nanorod arrays is perpendicular with that of the substrate. The average thickness of the nanorod arrays was roughly 1.52 μm. The diameter and thickness of the nanorod arrays might be controlled by varying the growth time, growth temperature, acidity of the solution, and concentration of titanium precursor, which was previously reported for hydrothermally grown TiO₂ nanorod arrays [5]. Both diameter and thickness of the nanorod arrays prepared by this technique are expected to change through the variation of experimental conditions as proven by previous studies on ZnO nanorod arrays, which also prepared using the Schott bottle [6,7]. The topographical AFM images in Fig. 2 (d) showed a similar pattern; the top view was obtained through FESEM, and the measured root mean square roughness, R_{rms} and average roughness, R_a of the synthesized TiO₂ were approximately 38.52 and 30.37 nm, respectively. However, these measured roughness values might not be accurate due to the existence of void between the nanorods and limitation of the probe tip to measure the individual nanorods down to the bottom side. These roughness values could be corrected by using the equations below [8]:

$$R_{rms}^* = \frac{T}{Z} R_{rms}, \quad (1)$$

$$R_a^* = \frac{T}{Z} R_a. \quad (2)$$

where R_{rms}^* is the corrective root mean square roughness, R_a^* is the corrective average roughness, T is the average thickness of the nanorod arrays, Z is the maximum z-range of the AFM probe tip (in our case, $Z=190$ nm), R_{rms} is the measured root mean square roughness from AFM, and R_a is the measured average roughness from AFM. From these equations, the calculated R_{rms}^* and R_a^* were 308 and 243 nm, respectively.

The chemical reactions are based on the dissolution condensation growth on the surface of the substrate. The resultant proposed growth of TiO₂ nanorod arrays is expressed as follows [9]:



where $R = \text{C}_4\text{H}_9$.

The hydrolysis reaction (Eq. (3)) removes four carbon atoms from the titanium precursor to form titanium hydroxyl; moreover, the condensation reaction (Eq. (4)) yields TiO₂ on the substrate and loses water. The rapid reactions are stabilized by HCl to avoid the immediate formation of precipitates or of large aggregates while preparing the aqueous solution. The ratio of DI water and HCl is important to control because this ratio affects the titanium alkoxide content for nanorod growth.

Fig. 3(a) exhibits the XRD result of the synthesized TiO₂ nanorod arrays. Without any other peaks to indicate the presence of the anatase and brookite phases of TiO₂, the detected peaks at (101), (210), (211), (002), (310), and (112) planes designate the tetragonal rutile structure of TiO₂ (JCPDS No. 01-072-1148). Based on the XRD pattern, the synthesized TiO₂ nanorod arrays exhibit polycrystalline structure as suggested by the appearance of multiple diffraction peaks, which correspond to the different plane orientations. SnO₂ peaks are also observed because of the X-ray penetration into the FTO-coated glass substrate. The structural phase of the synthesized TiO₂ nanorod arrays were also analyzed via micro-Raman spectroscopy, as shown in Fig. 3(b). Intense Raman peaks are detected at 445 and 609 cm⁻¹ for the E_g and A_{1g} modes, respectively. This finding confirms the rutile phase of TiO₂ and is consistent with the attained XRD result.

Fig. 4(a) illustrates the optical absorbance spectrum of TiO₂ nanorod arrays in a range of 200–800 nm. This spectrum indicates that the synthesized TiO₂ displays intense absorbance at less than 400 nm in the UV region; thus, these arrays can merely absorb UV wavelengths below this point. Fig. 4(b) depicts Tauc's plot of the TiO₂ nanorod arrays for optical band gap energy estimation, which was derived using the equation below:

$$\alpha h\nu = A(h\nu - E_g)^{1/2}, \quad (5)$$

where α is the absorption coefficient, $h\nu$ is the photon energy, A is a constant, and E_g is the bandgap energy. The extrapolation of the linear side of the graph indicates that the optical band gap energy falls at 3.2 eV, which is in the range of the TiO₂ rutile phase.

I - V is measured for the TiO₂ nanorods deposited at ambient temperature in a range of -1.5–1.5 V, as displayed in Fig. 4(c). A linear function exhibits an Ohmic characteristic in this voltage region at a resistivity of $7.0 \times 10^6 \Omega \text{ cm}$. Fig. 4(d) shows the time-dependent photocurrent property of the synthesized TiO₂ under 365 nm UV illumination at a bias voltage of 1 V in a sodium sulfate (Na₂SO₄) electrolyte solution. The photocurrent is increased at an average of 0.1 mA during UV irradiation and decreased after the

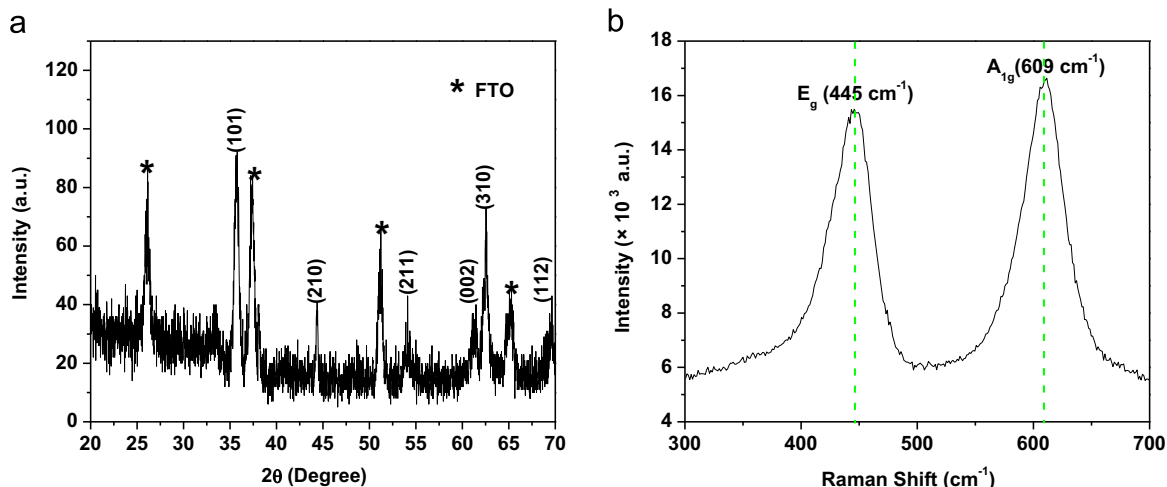


Fig. 3. (a) XRD pattern and (b) Raman spectrum of the rutile-phased TiO₂ nanorod arrays.

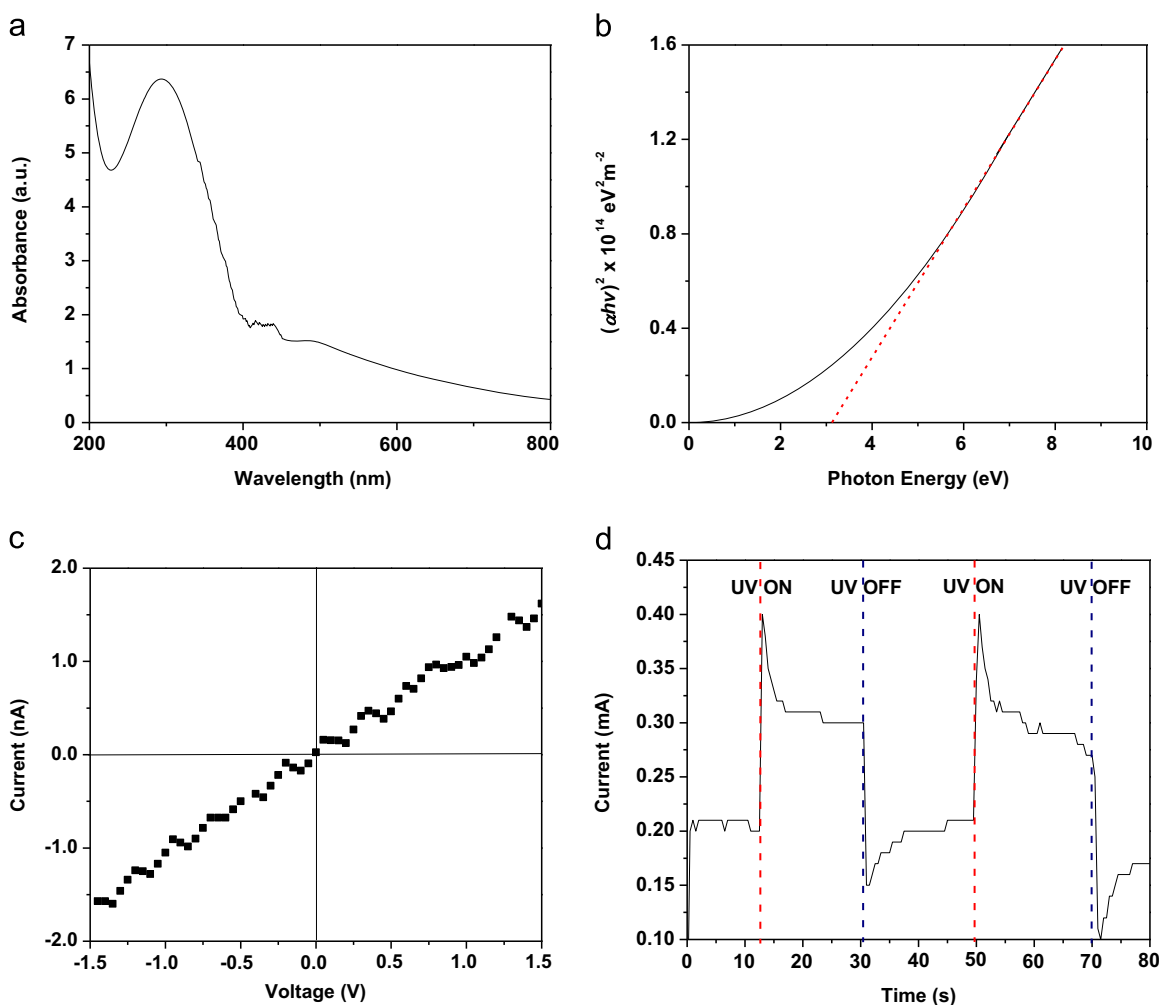


Fig. 4. (a) UV-vis absorbance spectrum, (b) Tauc's plot, (c) I - V characteristic, and (d) photocurrent response under UV irradiation (365 nm, 1 V bias) of synthesized TiO₂ nanorod arrays.

UV light is turned off. This behavior is attributed to the excitation of the photogenerated electron from the valence band into the conduction band through UV irradiation; as a result, the measured current increases. The rapid change observed in the current was in line with the fast response time of the fabricated TiO₂. Therefore, these electrical properties of synthesized TiO₂ facilitate the potential application of such arrays in low-power photosensors.

4. Conclusions

TiO₂ nanorod arrays were synthesized on a FTO-coated glass substrate through a facile aqueous chemical route via dissolution condensation growth in a low-cost Schott bottle with cap clamps. Uniform and dense TiO₂ nanorod arrays were obtained after 2 h of immersion; these synthesized arrays have an average diameter of 120 nm and an average length of 1.52 μm. XRD reveals that the sample is a crystalline TiO₂ in rutile phase, and our results demonstrate that the TiO₂ nanorod arrays respond well to 365-nm UV illumination in a Na₂SO₄ electrolyte solution. In conclusion, synthesized TiO₂ nanorod arrays are a promising material for photosensor applications.

Acknowledgment

This work was supported by the Long-Term Research Grant Scheme (600-RMI/LRGS 5/3 (3/2013)) and the Research Acculturation Collaborative Effort (RACE) Grant (600-RMI/RACE 16/6/2 (9/2013)) from the Ministry of Higher Education Malaysia. The authors would also like to thank the Research Management Institute (RMI) of UiTM and the International Islamic University of Malaysia (IIUM) for their financial support. Moreover, this research was assisted by the Research Chair of Targeting and Treatment of Cancer Using Nanoparticles, the Deanship of Scientific Research at King Saud University, Riyadh, Kingdom of Saudi Arabia. In addition, the authors acknowledge the College of Science of King Saud University, Riyadh, Kingdom of Saudi Arabia for the research collaboration.

References

- [1] M. Wang, C. Chen, B. Zhao, Q. Zeng, D. He, Solvothermal synthesis of nanostructured TiO₂ photocatalyst in supercritical CO₂ fluids, *Mater. Lett.* 109 (2013) 104–107.
- [2] C. Cao, C. Hu, X. Wang, S. Wang, Y. Tian, H.U.V. Zhang, sensor based on TiO₂ nanorod arrays on FTO thin film, *Sens. Actuators B* 156 (2011) 114–119.
- [3] H.-y Yang, X.-L. Cheng, X.-F. Zhang, Z.-k Zheng, X.-f Tang, Y.-M. Xu, et al., A novel sensor for fast detection of triethylamine based on rutile TiO₂ nanorod arrays, *Sens. Actuators B* 205 (2014) 322–328.
- [4] C. Fàbrega, T. Andreu, A. Tarancón, C. Flox, A. Morata, L. Calvo-Barrio, et al.,

- Optimization of surface charge transfer processes on rutile TiO₂ nanorods photoanodes for water splitting, *Int. J. Hydrog. Energy*. 38 (2013) 2979–2985.
- [5] B. Liu, E.S. Aydil, Growth of oriented single-crystalline rutile TiO₂ nanorods on transparent conducting substrates for dye-sensitized solar cells, *J. Am. Chem. Soc.* 131 (2009) 3985–3990.
- [6] M.H. Mamat, M.F. Malek, N.N. Hafizah, Z. Khusaimi, M.Z. Musa, M. Rusop, Fabrication of an ultraviolet photoconductive sensor using novel nanostructured, nanohole-enhanced, aligned aluminium-doped zinc oxide nanorod arrays at low immersion times, *Sens. Actuators B* 195 (2014) 609–622.
- [7] M.H. Mamat, Z. Khusaimi, M.M. Zahidi, A.B. Suriani, Y.M. Siran, S.A.M. Rejab, et al., Controllable growth of vertically aligned aluminum-doped zinc oxide nanorod arrays by sonicated sol–gel immersion method depending on precursor solution volumes, *Jpn. J. Appl. Phys.* 50 (2011) 06GH4.
- [8] A.G. Kontos, A.I. Kontos, D.S. Tsoukleris, V. Likodimos, J. Kunze, P. Schmuki, et al., Photo-induced effects on self-organized TiO₂ nanotube arrays: the influence of surface morphology, *Nanotechnology* 20 (2009) 045603.
- [9] P.D. Cozzoli, A. Kornowski, H. Weller, Low-temperature synthesis of soluble and processable organic-capped anatase TiO₂ nanorods, *J. Am. Chem. Soc.* 125 (2003) 14539–14548.